

UCSF

UC San Francisco Previously Published Works

Title

MicroRNA-10 regulates the angiogenic behavior of zebrafish and human endothelial cells by promoting vascular endothelial growth factor signaling.

Permalink

<https://escholarship.org/uc/item/8620w9fn>

Journal

Circulation Research, 111(11)

Authors

Hassel, David

Cheng, Paul

White, Mark

et al.

Publication Date

2012-11-09

DOI

10.1161/CIRCRESAHA.112.279711

Peer reviewed



Published in final edited form as:

Circ Res. 2012 November 9; 111(11): 1421–1433. doi:10.1161/CIRCRESAHA.112.279711.

miR-10 Regulates the Angiogenic Behavior of Zebrafish and Human Endothelial Cells by Promoting VEGF Signaling

David Hassel^{1,7}, Paul Cheng^{1,2,3,4}, Mark P. White^{1,2,3,4}, Kathryn N. Ivey^{1,2,3}, Jens Kroll^{5,6}, Hellmut G. Augustin^{5,6}, Hugo A. Katus⁷, Didier Y.R. Stainier^{4,8}, and Deepak Srivastava^{1,2,3,4}

¹Gladstone Institute of Cardiovascular Disease, San Francisco, CA 94158, USA

²Roddenberry Center for Stem Cell Biology and Medicine at Gladstone, San Francisco, CA, 94158, USA

³Department of Pediatrics, University of California, San Francisco, San Francisco, CA 94143, USA

⁴Department of Biochemistry & Biophysics, University of California, San Francisco, San Francisco, CA 94158, USA

⁵Department of Vascular Biology and Tumor Angiogenesis, Center for Biomedicine and Medical Technology Mannheim, Mannheim, Germany

⁶Division of Vascular Oncology and Metastasis, German Cancer Research Center (DKFZ-ZMBH Alliance), Heidelberg, Germany

⁷Department of Medicine III, Cardiology, University of Heidelberg, 69120 Heidelberg, Germany

⁸Department of Developmental Genetics, Max Planck Institute for Heart and Lung Research, 61231 Bad Nauheim, Germany

Abstract

Rationale—Formation and remodeling of the vasculature during development and disease involves a highly conserved and precisely regulated network of attractants and repellants. Various signaling pathways control the behavior of endothelial cells, but their post-transcriptional dose-titration by miRNAs is poorly understood.

Objective—To identify miRNAs that regulate angiogenesis.

Methods and Results—We show that the highly conserved microRNA family encoding miR-10 regulates the behavior of endothelial cells during angiogenesis by positively titrating pro-angiogenic signaling. Knockdown of miR-10 led to premature truncation of intersegmental vessel growth (ISV) in the trunk of zebrafish larvae, while overexpression of miR-10 promoted angiogenic behavior in zebrafish and cultured human umbilical venous endothelial cells (HUVECs). We found that miR-10 functions, in part, by directly regulating the level of fms-related tyrosine kinase 1 (FLT1), a cell-surface protein that sequesters VEGF, and its soluble splice variant sFLT1. The increase in FLT1/sFLT1 protein levels upon miR-10 knockdown in

Address correspondence to: Dr. Deepak Srivastava, Gladstone Institute of Cardiovascular Disease, University of California, San Francisco, 1650 Owens Street, San Francisco, CA, 94158, Tel: 415-734-2716, Fax: 415- 355-0141, dsrivastava@gladstone.ucsf.edu; Dr. David Hassel, Gladstone Institute of Cardiovascular Disease, University of California, San Francisco, 1650 Owens Street, San Francisco, CA, 94158, Tel: 415-734-2716, Fax: 415- 355-0141, david.hassel@med.uni-heidelberg.de.

Publisher's Disclaimer: This is a PDF file of an unedited manuscript that has been accepted for publication. As a service to our customers we are providing this early version of the manuscript. The manuscript will undergo copyediting, typesetting, and review of the resulting proof before it is published in its final citable form. Please note that during the production process errors may be discovered which could affect the content, and all legal disclaimers that apply to the journal pertain.

zebrafish and in HUVECs inhibited the angiogenic behavior of endothelial cells largely by antagonizing VEGF receptor-2 signaling.

Conclusion—Our study provides insights into how FLT1 and VEGF receptor-2 signaling is titrated in a miRNA-mediated manner and establishes miR-10 as a potential new target for the selective modulation of angiogenesis.

Keywords

microRNA; angiogenesis; developmental biology; VEGF; fms-related tyrosine kinase 1

INTRODUCTION

The circulatory system consists of a highly organized network of blood vessels that distributes nutrients, gases, and hormones throughout the body. Its formation is highly conserved and requires the coordination of two distinct cellular processes. During embryonic development, proliferating endothelial precursor cells migrate and differentiate in response to regional signaling cues to form a primitive lumenized vascular plexus, a process known as vasculogenesis. Through angiogenesis, this plexus is remodeled and extended by new blood vessel growth and addition of smooth muscle cells and pericytes.

In addition to regulating various physiological processes, such as development, organ growth, and immune and injury responses, the vasculature is involved in several pathophysiological conditions, including diabetic retinopathy and tumor growth.¹ Strategies targeting angiogenesis have proven to be valuable therapeutic approaches in preventing tumor progression.²

The establishment and remodeling of the vascular system depends on a precisely orchestrated interplay of attractants and repellants, in which several secreted signaling molecules—including vascular endothelial growth factor (VEGF), fibroblast growth factor (FGF), and platelet-derived growth factor (PDGF)—and their corresponding receptors transduce downstream signaling events that subsequently result in the modulation of endothelial cell behavior. The most potent of these angiogenic signaling factors, VEGF, functions by binding to one of three cognate receptor tyrosine kinases (VEGFR1-3).^{3, 4} Gene-targeting approaches in mice demonstrated a particularly important role for VEGFR2 (a.k.a, kinase insert domain receptor, KDR) in VEGF-mediated signaling, since VEGFR2-null mice die at embryonic day (E) 8.5–9 due to defective blood-island formation and the near-absence of vasculature.⁵ Stimulation of KDR with VEGF results in KDR autophosphorylation and activation of several well-studied signal transduction pathways.

In contrast, the role of VEGFR1 (or fms-related tyrosine kinase 1, FLT1) during vessel formation remains controversial. In mice, depletion of FLT1 results in early embryonic lethality at E8.5–9 due to increased hemangioblast commitment and disorganized blood vessel development as a result of endothelial cell overgrowth and excessive KDR activation, suggesting that FLT1 and its soluble splice variant sFLT1 (containing the extracellular VEGF binding domain only) negatively regulate KDR signaling.^{6, 7} In support of this concept, KDR phosphorylation levels are increased in embryonic stem cells (ESCs) lacking FLT1⁸. Despite a 10-fold higher affinity for VEGF than KDR, the level of FLT1 phosphorylation following VEGF exposure is extremely low.⁹ Mice lacking the kinase domain of FLT1 develop normal vasculature, further supporting the idea that FLT1 fine-tunes KDR signaling by sequestering VEGF and preventing it from binding to KDR.^{9, 10} While KDR and FLT1 seem to be important for vascular endothelial cell development, various genetic studies implicated a particularly important role for VEGFR3 (FLT-4) in establishing and maintaining lymphatic endothelial cells.^{11, 12} In blood endothelial cells,

VEGFR3/FLT-4 functions mainly in arterial/venous endothelial cell determination during intersegmental vessel sprouting through its ligand VEGF-C.^{13, 14}

In light of the complexity among angiogenic and anti-angiogenic stimuli, careful balancing of signals that control endothelial cell behavior is essential for the establishment, maintenance, and remodeling of the vasculature.¹⁵ In addition to known proteins that regulate downstream kinase-activation cascades, the post-transcriptional titration of key angiogenic signaling nodes by microRNAs (miRNAs) has gathered particular interest.¹⁶ miRNAs are small, single-stranded, endogenous non-coding RNAs averaging 22 nucleotides in length. miRNAs bind to target mRNAs based on sequence complementarity as well as accessibility of the potential target site, and negatively regulate gene expression by either translational inhibition or destabilization of target mRNAs.¹⁷ Several miRNAs regulate angiogenic signaling, including miR-126, members of the miR-17-92 cluster and miR-21.^{18–20}

miR-10 function is dysregulated in various cancers, where it was implicated in mediating tumor invasion and metastasis by altering the levels of its target, HOXD10.^{21, 22} However, little is known about its function in endothelial cells. Fang et al. recently demonstrated an involvement for miR-10 in regulation of the proinflammatory response in athero-susceptible endothelium by directly targeting key regulators of NF- κ B activation.²³ Additionally, Shen et al. demonstrated a role for miR-10b in regulating angiogenesis specifically in response to thrombin through down-regulation of HOXD10.²⁴ Here, we describe a novel role for miR-10 in modulating the angiogenic behavior of endothelial cells during development, in part through direct regulation of FLT1 and its soluble splice isoform sFLT1.

METHODS

Care and breeding of zebrafish (*Danio rerio*) was carried out essentially as described.²⁵ The *Tg(kdrl:EGFP)^{s843}* and *Tg(kdrl:nlsEGFP^{zfl109})*, *Tg(kdrl:HsHRAS-mCherry^{s896})*^{26, 27} strains were used. For immunofluorescence analysis in zebrafish, we used anti-MF20 (Developmental Studies Hybridoma Bank; 1:5) and anti-znp1 (Developmental Studies Hybridoma Bank; 1:100) antibodies.

Human umbilical vein endothelial cells (HUVECs) and recommended medium were purchased from ScienCell and cultured according to manufacturer's recommendations.

Undifferentiated mouse ESCs were propagated on gelatin-coated cell culture plastic (Nunc) in GMEM supplemented with 10% FBS, 0.1 mM nonessential amino acids, 2 mM GlutaMAX, 0.1 mM sodium pyruvate (Invitrogen), 0.1 mM 2-mercaptoethanol (Sigma-Aldrich), and 1500 U/ml leukemia inhibitory factor (LIF, Millipore). ES cells were passaged every 2–3 days with TrypLE Express (Invitrogen) with daily medium changes. ESC were dissociated to single cells and differentiated as embryoid bodies in ultra-low attachment plates (Corning) in GMEM supplemented with penicillin/streptomycin, 2 mM GlutaMAX, 0.1 mM nonessential amino acids (Sigma-Aldrich), and 20% FBS at a final concentration of 100,000 cells/ml.

The following antibodies were used: anti-Flk1 (BD Pharmigen 560680), anti-VE-Cad (Ebio-17-1441), anti-FLT1 (abcam; 1:500), anti-KDR (Cell Signaling; 1:2000), anti-phospho-KDR (Cell Signaling; 1:1000), anti-GAPDH (Santa Cruz; 1:2000), and anti-HOXD10 (Santa Cruz; 1:200), anti-phosphohistone H3 (Cell Signaling; 1:200), anti-Annexin V (Abcam; 1:200). For phospho-KDR western blots, HUVEC were serum-starved overnight and then treated with 2 or 10 ng/ml as indicated of human recombinant VEGF (BD Biosciences) for 10 min.

For all other experimental details see the Online Supplement at <http://circres.ahajournals.org>.

RESULTS

miR-10 expression is induced after mesoderm specification in ESCs and is enriched in KDR⁺ Cells

The miR-10a/10b isoforms are encoded in a highly conserved location within the developmental regulator cluster of HOX genes, a feature shared only by miR-196 and miR-615 (Online Figure I).^{28, 29} To determine when miR-10 expression is induced during early development, we assayed miR-10a and miR-10b expression, along with several marker genes, by quantitative reverse-transcriptase PCR (qRT-PCR), using mRNA derived from embryoid bodies (EB) at progressive stages of differentiation from mouse ESCs (Figure 1A, B). *Brachyury* (*Bry*), a marker of early mesoderm, was dramatically induced at day 4 of differentiation (D4), as was *Sox17*, a marker of endoderm (Figure 1A). Expression of miR-10a and miR-10b was significantly upregulated after mesoderm and endoderm induction at D6 (Figure 1B). Interestingly, *KDR/VEGFR2* expression was similarly induced at D6 and further increased until D10, suggesting that miR-10 might get induced in differentiating KDR-positive populations. During mESC differentiation, miR-10a was expressed more abundantly than miR-10b (Figure 1B). The cardiomyocyte marker *Myh7* was robustly detected at D8 (Figure 1A).

We next tested whether miR-10 might be expressed and enriched in endothelial cells, and found that miR-10a, but not miR-10b was almost 3.4-fold enriched in KDR/VE-Cadherin-positive endothelial cells compared to KDR/VE-Cadherin-negative non-endothelial cells (Figure 1C).

miR-10 regulates angiogenesis in vivo

Zebrafish express up to four miR-10 isoforms (miR-10a-d) encoded in five independent transcripts (Figure 2A). By qRT-PCR, we found that expression of all four isoforms was induced at 14 hpf and peaked at 20 hpf (Figure 2B). By 24 and 48 hpf, miR-10a and miR-10b levels had fallen while the expression levels of miR-10c and miR-10d were similar to those found at 14 hpf (Figure 2B).

To investigate loss-of-function effects during development, we injected two unique morpholino-modified oligonucleotide mixtures (MO-miR-10, MO-miR-10*) into one-cell-stage zebrafish embryos (Figure 2C). MO-miR-10 consists of two morpholinos that block the processing of pri-miR-10a and pri-miR-10b-1, resulting in profoundly reduced levels of mature miR-10a and miR-10b and, due to high homology, miR-10c and miR-10d (Figure 2A, D). MO-miR-10* consists of four morpholinos that target pre-miR-10 star isoforms (Figure 2A), which affect the processing of both the mature miRNA and its corresponding star isoform.³⁰ Injecting MO-miR-10* decreased mature miR-10 levels similar to MO-miR-10, demonstrating the specificity of both morpholinos (Figure 2D). Importantly, the level of zebrafish *hoxb4a*, where miR-10c resides intronically, was not appreciably altered by miR-10 morpholinos (Figure 2D).³¹ Reduction of miR-10 levels by MO-miR-10 or MO-miR-10* led to identical angiogenic phenotypes (Online Figure II). Because injection of MO-miR-10 was slightly more efficient in decreasing mature miR-10 levels and led to a more robust phenotype, all subsequent experiments were carried out with this morpholino mixture.

At 72 hpf, MO-miR-10-injected and control-injected embryos had no differences in gross morphology (Figure 2C, top row). Examination of transgenic zebrafish expressing GFP under the control of an endothelial-specific promoter, which marks the vasculature

[*Tg(kdrl:EGFP)^{s843}*] revealed that tail blood vessel formation was strongly affected by MO-miR-10-injection (Figure 2C).

The intersegmental vessels (ISV) in the zebrafish tail first sprout from the dorsal aorta (DA) and subsequently grow dorsally to form the dorsal longitudinal anastomotic vessel (DLAV). By 72 hpf, the ISVs in control embryos are nicely aligned and fully developed (Figure 2C, bottom row).³² In contrast, in miR-10-deficient embryos, approximately 6% of ISVs completely failed to sprout, while 50% of the sprouting ISVs stopped at the horizontal myoseptum, instead forming an ectopic longitudinal anastomotic vessel (ELAV) centered along the midline (Figure 2C, 2E). Furthermore, although some ISVs in MO-miR-10-injected embryos showed proper growth, 80% of all scored miR-10-deficient ISVs displayed defective formation of the DLAV (Figure 2C, 2E).

miR-10 also regulates the expression of several Hox genes.^{21, 31, 33} Hox gene function is essential for correct anterior-posterior patterning and normal somite morphogenesis during embryogenesis. Since dysmorphic or mispatterned somites can cause vascular defects, we evaluated whether miR-10-deficient embryos developed normal somites.^{34, 35} Immunolabeling of myosins in the somites (Online Figure III) and synaptotagmin-2 in motoneurons (Online Figure II) revealed normal somite boundaries and overall v-shaped appearance in miR-10-deficient embryos³⁶.

Knockdown of miR-10 affects angiogenic behavior of HUVECs in vitro

The high conservation of miR-10 between zebrafish and humans enabled us to use a single zebrafish morpholino to block processing of pre-miR-10 into mature miR-10 in HUVECs (Figure 2A and Online Figure I). Electroporation of this morpholino significantly decreased both mature miR-10a and miR-10b levels (Figure 3A). Importantly, mRNA levels of *Hoxd3*, where miR-10b is intronically encoded and which spans the *Hoxd4* locus, were unaffected (Figure 3A).

VEGF exposure significantly increased cell number in serum-starved control but not miR-10-deficient HUVECs (Figure 3B), while transfection of a miR-10 mimic enhanced cell proliferation in response to VEGF compared to mock-transfected cells. Immunostaining for the cell death marker Annexin V confirmed that miR-10-deficient HUVECs did not display increased cell death, suggesting that miR-10 affects VEGF-mediated cell proliferation (Figure 3C). To assess how miR-10 depletion affects the angiogenic potential of HUVECs, we used a matrigel capillary tube formation assay to assess sprouting activity and capillary network complexity. miR-10 deficiency in HUVECs resulted in significantly shorter tube length and fewer branching points after 24 h than in control cells, indicating overall reduced angiogenic potential (Figure 3D). Interestingly, overexpression of miR-10 led to similar tube lengths as observed in control but significantly more sprouting and branching activity (Figure 3D). Furthermore, lentiviral-mediated knockdown of miR-10 decreased angiogenic potential in a HUVEC three-dimensional spheroid-based sprouting assay (Figures 4A and Online Figure VIIA). We next examined migratory potential following VEGF exposure using the scratch (wound-closure) assay. In control-transfected confluent HUVEC cultures, cells quickly began to migrate into the cell-cleared area after the scratch, and the wound closed 28±10% by 8 h and 70±10% after 24 h. In contrast, cell migration into the wound area of miR-10-deficient HUVECs was severely reduced, with only 17±2% (p<0.05) at 8 h and 30±7% closure by 24 h (p<0.0002) (Figure 3E). Conversely, overexpression resulted in a significantly increased migratory behavior, with 30±11% and 84±10% wound closure at 8 and 24 h, respectively (Figure 3E). Furthermore, kinetic measurements of cell attachment revealed significantly lower adhesion of MO-miR-10-deficient HUVECs than controls (Online Figure IV).

To evaluate whether miR-10-deficient HUVECs also display less angiogenic potential in situ, we engrafted control and miR-10-knockdown cells subcutaneously into mice using a matrigel xenografting assay.^{37, 38} The reduction of miR-10 in the HUVEC xenograft resulted in decreased mean vessel density compared to control-transduced cells ($p < 0.05$) (Figure 4B).

miR-10 deficiency affects endothelial cell behavior in vivo

Since miR-10 depletion significantly affected human endothelial cell behavior, we evaluated its effects in vivo in double transgenic zebrafish that expressed nuclear-localizing GFP and cytoplasmic mCherry in all endothelial cells of the vasculature [*Tg(kdrl:nlsEGFP^{zfl109}*; *Tg(kdrl:HsHRAS-mCherry^{s896})*]. In scrambled control-MO-injected embryos, ISV cells emerged from the DA at around 20 hpf and migrated dorsally. At 24 hpf, the majority of control ISVs consisted of two ($49.96 \pm 12\%$) or three ($34.16 \pm 7\%$) endothelial cells evenly distributed over the length of the ISV from the DA to approximately the level of the horizontal myoseptum (Figure 5A, B). Thereafter, ISVs continued to migrate until they reached the dorsal roof of the zebrafish tail, where they formed the DLAV at approximately 30 hpf. At 48 hpf, the majority of ISVs consisted of four ($53.2 \pm 10\%$) or five ($31.89 \pm 11\%$) endothelial cells, evenly distributed between the DA and the DLAV (Figure 5A, C). In 24 hpf miR-10-deficient embryos, most ISVs reached the horizontal myoseptum, although some ISVs failed to sprout (Figure 5A). However, most had significantly fewer cells/ISV (Figure 5B). At 48 hpf, most ISVs in MO-miR-10-injected embryos grew only halfway, halting at the horizontal myoseptum, with the majority of ISVs consisting of two endothelial cells ($48.9 \pm 11\%$) (Figure 5A, C). Notably, endothelial cells aggregated within ISVs and were seemingly unable to separate during dorsal migration, suggesting defective migration (Figure 5A).

To determine if miR-10 overexpression could promote angiogenic behavior in vivo, we injected miR-10 mimic into *Tg(kdrl:EGFP)^{s843}* transgenic fish. miR-10 overexpression had no obvious morphological defects (Figure 5D), and overall angiogenesis appeared normal. However, by 48hpf, zebrafish expressing excess miR-10 developed pericardial edema accompanied by blood congestion at the inflow tract, indicative of cardiac dysfunction (Figure 5D). Interestingly, *Tg(kdrl:nlsEGFP^{zfl109}*; *Tg(kdrl:HsHRAS-mCherry^{s896})* embryos overexpressing miR-10 revealed a significant increase in endothelial cells/ISV at 50 hpf (Figure 5E,F), indicating that miR-10-overexpressing endothelial cells have enhanced angiogenic potential in vivo.

miR-10 directly modulates FLT1 levels post-transcriptionally

To understand the molecular mechanism by which miR-10 modulates endothelial cell behavior, we searched for direct miR-10 targets using microRNA prediction programs, including an algorithm developed in our laboratory that integrates sequence complementarity and mRNA target site accessibility (unpublished data). We cloned the 3'UTR of putative targets containing the possible miR-10 binding site into the 3'UTR of a luciferase construct and tested the ability of miR-10 to repress luciferase expression in COS-7 cells. We chose the 3'UTR of the validated miR-10 target HOXD10 as a positive control and tested the 3'UTRs of FLT1, its soluble splice variant sFLT1 and Sprouty 4 (Spry4), based on binding sites and their known function in regulating endothelial cell biology.^{21, 39, 40} miR-10 significantly repressed the expression of luciferase constructs containing the 3'UTR of HOXD10, FLT1, and sFLT1 but not SPRY4 (Figures 6A, B and S6). Importantly, mutating the potential binding site for miR-10 in the 3'UTR of HOXD10, FLT1, and sFLT1 abolished miR-10-dependent repression of luciferase activity.

By qRT-PCR, we found that mRNA levels derived from miR-10-deficient HUVECs were unchanged; however, *FLT1* levels from MO-miR-10-injected zebrafish were significantly upregulated, suggesting differential effects of miR-10 on *FLT1* mRNA in humans and zebrafish (Figure 6C). Strikingly, FLT1 protein levels were dramatically upregulated in miR-10-deficient compared to control HUVECs (Figure 6D). Additionally, by ELISA we found a 3.4 ± 0.58 -fold ($p < 0.05$) increase in sFLT1 protein levels in the supernatant of MO-miR-10-transfected HUVECs compared to control-transfected cells (Figure 6E). These results clearly show that miR-10 directly targets the 3'UTR of FLT1 and sFLT1, and thereby titrates the level of FLT1/sFLT1 protein.

Increased FLT1 Levels in miR-10 deficiency antagonize KDR-dependent signaling

While much is known about VEGF receptor-2 (KDR) signaling and function in endothelial cells, comparatively little is known about the function of FLT1, although it is thought to function, in part, by preventing VEGF binding to KDR.^{6, 41} We hypothesize that KDR and FLT1 in a low-VEGF environment would compete for VEGF-binding and, due to the higher affinity of FLT1 for VEGF, that increasing FLT1 levels following miR-10 deficiency would result in decreased VEGF-KDR binding. We measured VEGF-mediated auto-phosphorylation of KDR in control or MO-miR-10-transfected HUVECs cultured with low levels of VEGF (2 ng/ml) and found that, indeed, knockdown of miR-10 caused a heterogeneous but significant decrease in KDR phosphorylation (Figure 6F). Interestingly, higher doses of VEGF (10 ng/ml) resulted in similar phosphorylation of KDR in miR-10-deficient HUVECs and controls, yet phenotypic defects persisted (Figures 6F and 3 B-E), suggesting that signaling downstream of FLT1 may also contribute to the observed anti-angiogenic effect.^{8, 39, 42, 43}

To test whether reduced KDR function might cause angiogenesis defects similar to miR-10-deficiency, we treated 20 hpf embryos, in which trunk vessels are already developed but ISVs have not started to sprout, with low doses of the VEGFR2-specific inhibitor SU5416.⁴⁴ At 30 hpf, inhibitor-treated embryos displayed blunted growth of ISVs stalled at the midline and significantly fewer endothelial cells per ISV (Figure 7A). Hence, pharmacological inhibition of KDR activity results in an angiogenic phenotype closely resembling miR-10 deficiency. To determine whether increased FLT1 and sFLT1 levels could induce angiogenesis defects similar to decreased miR-10 in vivo, we injected full-length FLT1 mRNA in zebrafish. This resulted in ISV profiles similar to KDR inhibition, consisting of predominantly two endothelial cells (Figure 7A). Increasing sFLT1 resulted in a more dramatic decrease in angiogenesis with significantly more ISVs consisting of only 0–1 cell/ISV, suggesting a more potent negative-regulatory potential of sFLT1 on pro-angiogenic KDR signaling compared to full-length FLT1 (Figure 7A). Thus, increased expression of FLT1 mimics many of the angiogenic defects of miR-10 inhibition. Importantly, arterial and venous gene expression (Online Figure V) was unaffected upon miR-10 knockdown compared to control embryos, suggesting that reduced VEGF signaling in MO-miR-10-injected embryos did not alter arterial-venous fate in early vasculogenesis.^{8, 46}

Reducing FLT1 levels rescues miR-10 knockdown-induced defects in angiogenesis

If FLT1 levels contribute significantly to the defects seen in HUVECs and in zebrafish upon miR-10 knockdown, we hypothesized that reducing FLT1 protein levels could rescue miR-10 deficiency in endothelial cells. miR-10-deficient HUVECs transfected with an siRNA against human FLT1 responded to VEGF treatment with a noticeable increase in cell number, comparable to that observed in control cells (Figures 7B and Online Figure VII). Immunostaining against the cell proliferation marker phospho-histone H3 (PH3) revealed that reduction of FLT1 expression in miR-10-deficient HUVECs rescued VEGF-induced proliferation (Figure 7C). In vivo, we co-injected sub-phenotypic amounts of an established

FLT1 morpholino (MO-FLT1) together with MO-miR-10 and analyzed ISV formation at 36 hpf in *Tg(kdr:EGFP)^{s843}* embryos.⁴⁷ While only 19±5% (n = 185) of the embryos injected with MO-miR-10 alone showed normal ISVs, 63±3% (n = 196) of embryos co-injected with MO-FLT1 developed normal ISVs compared to 99±0.5% of all control embryos with normal ISVs (Figure 7E).

DISCUSSION

Here, we provide evidence that miR-10 regulates endothelial cell behavior and we demonstrate that loss of miR-10 severely affects angiogenesis in vivo. By directly targeting both FLT1 and its soluble splice isoform sFLT1, miR-10 functions to promote KDR-mediated signaling following VEGF exposure, and can titrate pro-angiogenic signaling to fine-tune endothelial cell proliferation, migration, and adhesion.

In zebrafish embryos, we found that loss of miR-10 stalls ISV growth during angiogenesis. ISVs in MO-miR-10-injected embryos had fewer endothelial cells than did controls, indicating reduced proliferation, while increasing miR-10 levels produced ISVs with more endothelial cells but without ISV hyperbranching. Pathfinding of dorsally growing ISVs is controlled somewhat independently of VEGF-A. For example, semaphorin-plexinD1 signaling from the adjacent somites acts repulsively to guide endothelial cells during ISV growth.⁴⁸ We do not have evidence that increased miR-10 alters these signals, consistent with sprout guidance not being affected in miR-10 overexpressing endothelial cells. However, similar to what was observed previously, augmented angiogenic potential in miR-10 overexpressing larvae expressed in increased proliferative response and thereby in increased endothelial cell number per ISV during angiogenesis, suggesting augmented angiogenic potential.⁴⁹ Furthermore, miR-10 deficiency in HUVECs disturbed angiogenic behavior in vitro, while increased miR-10 augmented some aspects of angiogenesis. Importantly, the angiogenic potential of miR-10-deficient HUVECs in a matrigel xenograft model was decreased, underscoring the importance of miR-10 in regulating angiogenesis.

We identified FLT1 and its soluble splice variant sFLT1 as direct targets of miR-10, and demonstrated that miR-10 depletion results in elevated FLT1 mRNA levels in zebrafish and increased FLT1 and sFLT1 protein levels in HUVECs. FLT1 is rigidly inserted in the plasma membrane and intrinsically modulates proliferation and migration, while sFLT1 functions extracellularly to spatially modulate VEGF availability and thereby regulate angiogenesis and vessel branching. Mice lacking FLT1 display endothelial cell overgrowth, blood vessel disorganization and hyper-phosphorylated KDR.⁶ Conversely, FLT1 activation causes defects in angiogenesis and endothelial cell proliferation in response to VEGF coincident with reduced KDR phosphorylation, indicating that FLT1 negatively modulates KDR-mediated pro-angiogenic signaling.^{8, 50}

In HUVECs, we showed that miR-10 depletion and low-dose VEGF stimulation led to decreased phosphorylation of KDR. This confirms that the upregulation of FLT1 and sFLT1 protein by miR-10 knockdown antagonizes KDR stimulation, most likely due to the higher affinity of both FLT1s for VEGF. Additionally, treatment with the KDR-specific inhibitor SU5416 mimicked the miR-10 knockdown phenotype in zebrafish, suggesting that the observed angiogenesis defects in miR-10-deficient zebrafish is caused by diminished KDR function.

Consistent with previous reports, we demonstrated that overexpression of FLT1 in zebrafish causes reduced ISV sprouting with vessels stalled halfway towards the dorsal root.⁵¹ This phenotype is identical to that of miR-10-depleted embryos, suggesting that FLT1/sFLT1 upregulation upon miR-10 knockdown critically contributes to the observed angiogenesis

defect. In addition to increased cell numbers per ISV, FLT1 deficiency can result in excessive segmental vessel branching, an effect we did not observe in miR-10 duplex injected larvae.⁵¹ This discrepancy is likely attributed to the fact that excess miR-10 causes hypomorphic effects by only moderately reducing, rather than completely depleting, FLT1, leaving sufficient protein to influence endothelial cell division without affecting vessel sprouting. Ultimately, the ability to partially rescue the vascular phenotype in miR-10-deficient embryos with concomitant reduction of FLT1 levels suggests that the abnormal angiogenic behavior in endothelial cells lacking miR-10 is, to a great extent, caused by the increase in FLT1 protein.

FLT1 is unlikely to be the only important direct target of miR-10 in endothelial cells, given that FLT1 knockdown incompletely rescues angiogenesis in MO-miR-10-injected zebrafish and incompletely restores proliferation in HUVECs lacking miR-10 at later stages. HOXD10 was described as a very important target of miR-10 in the context of cancer invasion and metastasis.²¹ In endothelial cells, HOXD10 overexpression can inhibit angiogenesis⁵², while Shen et al.²⁴ recently demonstrated that the known angiogenic or anti-angiogenic potential of thrombin or heparin, respectively, is mediated in part through regulation of miR-10b and HOXD10. Our data establish FLT1 as a novel target for miR-10 in endothelial cell biology during development and suggest that miR-10 co-regulates multiple targets to modulate the angiogenic behavior of vascular endothelial cells. Interestingly, recent reports showed that heparin treatment is accompanied by a strong induction of sFLT1 protein.^{53, 54}

We found that high-dose VEGF could not rescue the proliferation defect or the reduced angiogenic behavior of HUVECs lacking miR-10, despite the rescue of KDR phosphorylation. In mice, FLT1-depletion can be partially rescued by expressing an FLT1 variant lacking the tyrosine kinase domain.¹⁰ Furthermore, proliferation and branching of vessels derived from FLT1-mutant ESCs can be rescued by soluble sFLT1.^{8, 10, 43} These findings suggest that FLT1 predominantly functions as a sequestering receptor for VEGF, preventing it from binding to KDR, and that the tyrosine kinase domain may be dispensable for FLT1 function during early development. However, others showed that signaling downstream of FLT1 is particularly important for antagonizing KDR-mediated pro-angiogenic signaling without affecting KDR or MAPK phosphorylation.^{46, 55} Our data favor a dual role of FLT1/sFLT1 in (1) titrating the dose and spatial availability of VEGF, particularly through sFLT1, and (2) a distinct KDR-antagonizing signaling cascade downstream of FLT1. Further studies are needed to dissect the signaling events downstream of FLT1.

With miR-10, we provide evidence of a miRNA that fine-tunes the tightly balanced process of vascular formation by targeting an important growth factor receptor. Our study establishes miR-10 as an important new target to modulate angiogenesis. As FLT1, sFLT1, and miR-10 are expressed in various tissues and are proposed to be involved in the pathogenesis of various diseases including cancer, studies linking miR-10 levels with FLT1 expression in diseased tissues could provide further mechanistic insights and open new opportunities for novel therapeutic approaches.⁵⁶⁻⁵⁸

Supplementary Material

Refer to Web version on PubMed Central for supplementary material.

Acknowledgments

We thank G. Howard & A.L. Lucido for editorial assistance, B. Taylor for manuscript and figure preparation, members of the Srivastava lab for helpful comments, K. Thorn from the Nikon Imaging Center at UCSF and U.

Engel and N. Dross from the Nikon Imaging Center at the University of Heidelberg. Special thanks goes to L. Juergensen for excellent technical assistance.

SOURCES OF FUNDING

D.H. was supported by the Deutsche Forschungsgemeinschaft (DFG; HA 5819/1-1) and the German Center for Cardiovascular Diseases (DZHK). K.N.I. was supported by grants from the American Heart Association and the California Institute for Regenerative Medicine (CIRM). D.Y.R.S. was supported by grants from the NIH (HL54737) and the Packard Foundation. D.S. was supported by grants from NHLBI/NIH (U01 HL100406), CIRM, the William Younger Family Foundation, the L.K. Whittier Foundation, and the Roddenberry Foundation. This work was supported by NIH-NIGMS (T32 GMO7618) to USCF MSTP, and NIH/NCRR grant (C06 RR018928) to the Gladstone Institute. Supported by grants from the Deutsche Forschungsgemeinschaft SFB-TR23 "Vascular Differentiation and Remodeling (project A3 to H.G.A. and project Z5 to J.K. H.G.A. is supported by an endowed Chair from the Aventis Foundation

DISCLOSURES

D.S. is on the Scientific Advisory Board of RegeneRx Biopharmaceuticals, Inc., and iPierian Inc.

Non-Standard Abbreviations

DA	dorsal aorta
DLAV	dorsal longitudinal anastomotic vessel
ELAV	ectopic longitudinal anastomotic vessel
HUVEC	human umbilical venous endothelial cells
ISV	intersegmental vessel
kdr1	kdr-like
miR	microRNA
nls	nuclear localization signal
PCV	posterior cardinal vein
Tg	Transgene
hpf	hours post fertilization

References

1. Risau W. Mechanisms of angiogenesis. *Nature*. 1997; 386:671–674. [PubMed: 9109485]
2. Gibaldi M. Regulating angiogenesis: A new therapeutic strategy. *J Clin Pharmacol*. 1998; 38:898–903. [PubMed: 9807969]
3. Ferrara N, Carver-Moore K, Chen H, Dowd M, Lu L, O'Shea KS, Powell-Braxton L, Hillan KJ, Moore MW. Heterozygous embryonic lethality induced by targeted inactivation of the vegf gene. *Nature*. 1996; 380:439–442. [PubMed: 8602242]
4. Carmeliet P, Ferreira V, Breier G, Pollefeyt S, Kieckens L, Gertsenstein M, Fahrig M, Vandenhoeck A, Harpal K, Eberhardt C, Declercq C, Pawling J, Moons L, Collen D, Risau W, Nagy A. Abnormal blood vessel development and lethality in embryos lacking a single vegf allele. *Nature*. 1996; 380:435–439. [PubMed: 8602241]
5. Shalaby F, Rossant J, Yamaguchi TP, Gertsenstein M, Wu XF, Breitman ML, Schuh AC. Failure of blood-island formation and vasculogenesis in flk-1-deficient mice. *Nature*. 1995; 376:62–66. [PubMed: 7596435]
6. Fong GH, Zhang L, Bryce DM, Peng J. Increased hemangioblast commitment, not vascular disorganization, is the primary defect in flt-1 knock-out mice. *Development*. 1999; 126:3015–3025. [PubMed: 10357944]

7. Fong GH, Rossant J, Gertsenstein M, Breitman ML. Role of the flt-1 receptor tyrosine kinase in regulating the assembly of vascular endothelium. *Nature*. 1995; 376:66–70. [PubMed: 7596436]
8. Roberts DM, Kearney JB, Johnson JH, Rosenberg MP, Kumar R, Bautch VL. The vascular endothelial growth factor (vegf) receptor flt-1 (vegfr-1) modulates flk-1 (vegfr-2) signaling during blood vessel formation. *Am J Pathol*. 2004; 164:1531–1535. [PubMed: 1511299]
9. Seetharam L, Gotoh N, Maru Y, Neufeld G, Yamaguchi S, Shibuya M. A unique signal transduction from flt tyrosine kinase, a receptor for vascular endothelial growth factor vegf. *Oncogene*. 1995; 10:135–147. [PubMed: 7824266]
10. Hiratsuka S, Minowa O, Kuno J, Noda T, Shibuya M. Flt-1 lacking the tyrosine kinase domain is sufficient for normal development and angiogenesis in mice. *Proc Natl Acad Sci U S A*. 1998; 95:9349–9354. [PubMed: 9689083]
11. Makinen T, Jussila L, Veikkola T, Karpanen T, Kettunen MI, Pulkkanen KJ, Kauppinen R, Jackson DG, Kubo H, Nishikawa S, Yla-Herttuala S, Alitalo K. Inhibition of lymphangiogenesis with resulting lymphedema in transgenic mice expressing soluble vegf receptor-3. *Nat Med*. 2001; 7:199–205. [PubMed: 11175851]
12. Karkkainen MJ, Ferrell RE, Lawrence EC, Kimak MA, Levinson KL, McTigue MA, Alitalo K, Finegold DN. Missense mutations interfere with vegfr-3 signalling in primary lymphoedema. *Nat Genet*. 2000; 25:153–159. [PubMed: 10835628]
13. Hogan BM, Herpers R, Witte M, Helotera H, Alitalo K, Duckers HJ, Schulte-Merker S. Vegfc/flt4 signalling is suppressed by dll4 in developing zebrafish intersegmental arteries. *Development*. 2009; 136:4001–4009. [PubMed: 19906867]
14. Covassin LD, Villefranc JA, Kacergis MC, Weinstein BM, Lawson ND. Distinct genetic interactions between multiple vegf receptors are required for development of different blood vessel types in zebrafish. *Proc Natl Acad Sci USA*. 2006; 103:6554–6559. [PubMed: 16617120]
15. Carmeliet P. Angiogenesis in life, disease and medicine. *Nature*. 2005; 438:932–936. [PubMed: 16355210]
16. Fish JE, Srivastava D. Micrnas: Opening a new vein in angiogenesis research. *Sci Signal*. 2009; 2:pe1. [PubMed: 19126861]
17. Zhao Y, Samal E, Srivastava D. Serum response factor regulates a muscle-specific microrna that targets hand2 during cardiogenesis. *Nature*. 2005; 436:214–220. [PubMed: 15951802]
18. Sabatel C, Malvaux L, Bovy N, Deroanne C, Lambert V, Gonzalez ML, Colige A, Rakic JM, Noel A, Martial JA, Struman I. Microrna-21 exhibits antiangiogenic function by targeting rhob expression in endothelial cells. *PLoS One*. 2011; 6:e16979. [PubMed: 21347332]
19. Fish JE, Santoro MM, Morton SU, Yu S, Yeh RF, Wythe JD, Ivey KN, Bruneau BG, Stainier DY, Srivastava D. Mir-126 regulates angiogenic signaling and vascular integrity. *Dev Cell*. 2008; 15:272–284. [PubMed: 18694566]
20. Dews M, Homayouni A, Yu D, Murphy D, Seignani C, Wentzel E, Furth EE, Lee WM, Enders GH, Mendell JT, Thomas-Tikhonenko A. Augmentation of tumor angiogenesis by a myc-activated microrna cluster. *Nat Genet*. 2006; 38:1060–1065. [PubMed: 16878133]
21. Ma L, Teruya-Feldstein J, Weinberg RA. Tumour invasion and metastasis initiated by microrna-10b in breast cancer. *Nature*. 2007; 449:682–688. [PubMed: 17898713]
22. Ciafre SA, Galardi S, Mangiola A, Ferracin M, Liu CG, Sabatino G, Negrini M, Maira G, Croce CM, Farace MG. Extensive modulation of a set of micrnas in primary glioblastoma. *Biochem Biophys Res Commun*. 2005; 334:1351–1358. [PubMed: 16039986]
23. Fang Y, Shi C, Manduchi E, Civelek M, Davies PF. Microrna-10a regulation of proinflammatory phenotype in athero-susceptible endothelium in vivo and in vitro. *Proc Natl Acad Sci USA*. 2010; 107:13450–13455. [PubMed: 20624982]
24. Shen X, Fang J, Lv X, Pei Z, Wang Y, Jiang S, Ding K. Heparin impairs angiogenesis through inhibition of microrna-10b. *J Biol Chem*. 2011; 286:26616–26627. [PubMed: 21642433]
25. Westerfield, M. *The zebrafish book. A guide for the laboratory use of zebrafish (danio rerio)*. 3rd edition. Eugene, OR: University of Oregon Press; 1995. p. 385(Book)
26. Jin SW, Herzog W, Santoro MM, Mitchell TS, Frantsve J, Jungblut B, Beis D, Scott IC, D'Amico LA, Ober EA, Verkade H, Field HA, Chi NC, Wehman AM, Baier H, Stainier DY. A transgene-

- assisted genetic screen identifies essential regulators of vascular development in vertebrate embryos. *Dev Biol.* 2007; 307:29–42. [PubMed: 17531218]
27. Bussmann J, Bakkers J, Schulte-Merker S. Early endocardial morphogenesis requires *scl/tal1*. *PLoS Genet.* 2007; 3:e140. [PubMed: 17722983]
 28. Tanzer A, Amemiya CT, Kim CB, Stadler PF. Evolution of micrnas located within *hox* gene clusters. *J Exp Zool B Mol Dev Evol.* 2005; 304:75–85. [PubMed: 15643628]
 29. Lim LP, Glasner ME, Yekta S, Burge CB, Bartel DP. Vertebrate micrna genes. *Science.* 2003; 299:1540. [PubMed: 12624257]
 30. Kloosterman WP, Lagendijk AK, Ketting RF, Moulton JD, Plasterk RH. Targeted inhibition of mirna maturation with morpholinos reveals a role for *mir-375* in pancreatic islet development. *PLoS Biol.* 2007; 5:e203. [PubMed: 17676975]
 31. Woltering JM, Durston AJ. *Mir-10* represses *hoxb1a* and *hoxb3a* in zebrafish. *PLoS One.* 2008; 3:e1396. [PubMed: 18167555]
 32. Isogai S, Lawson ND, Torrealday S, Horiguchi M, Weinstein BM. Angiogenic network formation in the developing vertebrate trunk. *Development.* 2003; 130:5281–5290. [PubMed: 12954720]
 33. Garzon R, Pichiorri F, Palumbo T, Iuliano R, Cimmino A, Aqeilan R, Volinia S, Bhatt D, Alder H, Marcucci G, Calin GA, Liu CG, Bloomfield CD, Andreeff M, Croce CM. Micrna fingerprints during human megakaryocytopoiesis. *Proc Natl Acad Sci USA.* 2006; 103:5078–5083. [PubMed: 16549775]
 34. Shaw KM, Castranova DA, Pham VN, Kamei M, Kidd KR, Lo BD, Torres-Vasquez J, Ruby A, Weinstein BM. Fused-somites-like mutants exhibit defects in trunk vessel patterning. *Dev Dyn.* 2006; 235:1753–1760. [PubMed: 16607654]
 35. Schilling TF, Knight RD. Origins of anteroposterior patterning and *hox* gene regulation during chordate evolution. *Philos Trans R Soc Lond B Biol Sci.* 2001; 356:1599–1613. [PubMed: 11604126]
 36. van Eeden FJ, Granato M, Schach U, Brand M, Furutani-Seiki M, Haffter P, Hammerschmidt M, Heisenberg CP, Jiang YJ, Kane DA, Kelsh RN, Mullins MC, Odenthal J, Warga RM, Allende ML, Weinberg ES, Nusslein-Volhard C. Mutations affecting somite formation and patterning in the zebrafish, *danio rerio*. *Development.* 1996; 123:153–164. [PubMed: 9007237]
 37. Laib AM, Bartol A, Alajati A, Korff T, Weber H, Augustin HG. Spheroid-based human endothelial cell microvessel formation in vivo. *Nature Protocols.* 2009; 4:1202–1215.
 38. Alajati A, Laib AM, Weber H, Boos AM, Bartol A, Ikenberg K, Korff T, Zentgraf H, Obodozie C, Graeser R, Christian S, Finkenzeller G, Stark GB, Heroult M, Augustin HG. Spheroid-based engineering of a human vasculature in mice. *Nature Methods.* 2008; 5:439–445. [PubMed: 18391960]
 39. Kearney JB, Ambler CA, Monaco KA, Johnson N, Rapoport RG, Bautch VL. Vascular endothelial growth factor receptor *flt-1* negatively regulates developmental blood vessel formation by modulating endothelial cell division. *Blood.* 2002; 99:2397–2407. [PubMed: 11895772]
 40. Lee SH, Schloss DJ, Jarvis L, Krasnow MA, Swain JL. Inhibition of angiogenesis by a mouse sprouty protein. *J Biol Chem.* 2001; 276:4128–4133. [PubMed: 11053436]
 41. Roeckl W, Hecht D, Sztajer H, Waltenberger J, Yayon A, Weich HA. Differential binding characteristics and cellular inhibition by soluble *vegf* receptors 1 and 2. *Exp Cell Res.* 1998; 241:161–170. [PubMed: 9633524]
 42. Kappas NC, Zeng G, Chappell JC, Kearney JB, Hazarika S, Kallianos KG, Patterson C, Annex BH, Bautch VL. The *vegf* receptor *flt-1* spatially modulates *flk-1* signaling and blood vessel branching. *J Cell Biol.* 2008; 181:847–858. [PubMed: 18504303]
 43. Kearney JB, Kappas NC, Ellerstrom C, DiPaola FW, Bautch VL. The *vegf* receptor *flt-1* (*vegfr-1*) is a positive modulator of vascular sprout formation and branching morphogenesis. *Blood.* 2004; 103:4527–4535. [PubMed: 14982871]
 44. Chan J, Bayliss PE, Wood JM, Roberts TM. Dissection of angiogenic signaling in zebrafish using a chemical genetic approach. *Cancer Cell.* 2002; 1:257–267. [PubMed: 12086862]
 45. Herbert SP, Huisken J, Kim TN, Feldman ME, Houseman BT, Wang RA, Shokat KM, Stainier DY. Arterial-venous segregation by selective cell sprouting: An alternative mode of blood vessel formation. *Science.* 2009; 326:294–298. [PubMed: 19815777]

46. Zeng H, Zhao D, Mukhopadhyay D. Flt-1-mediated down-regulation of endothelial cell proliferation through pertussis toxin-sensitive G proteins, beta gamma subunits, small GTPase cdc42, and partly by Rac-1. *J Biol Chem.* 2002; 277:4003–4009. [PubMed: 11726672]
47. Rottbauer W, Just S, Wessels G, Trano N, Most P, Katus HA, Fishman MC. Vegfplcgamma1 pathway controls cardiac contractility in the embryonic heart. *Genes Dev.* 2005; 19:1624–1634. [PubMed: 15998812]
48. Torres-Vazquez J, Gitler AD, Fraser SD, Berk JD, Van NP, Fishman MC, Childs S, Epstein JA, Weinstein BM. Semaphorin-plexin signaling guides patterning of the developing vasculature. *Dev Cell.* 2004; 7:117–123. [PubMed: 15239959]
49. Nicoli S, Knyphausen CP, Zhu LJ, Lakshmanan A, Lawson ND. Mir-221 is required for endothelial tip cell behaviors during vascular development. *Dev Cell.* 2012; 22:418–429. [PubMed: 22340502]
50. Chappell JC, Taylor SM, Ferrara N, Bautch VL. Local guidance of emerging vessel sprouts requires soluble Flt-1. *Dev Cell.* 2009; 17:377–386. [PubMed: 19758562]
51. Krueger J, Liu D, Scholz K, Zimmer A, Shi Y, Klein C, Siekmann A, Schulte-Merker S, Cudmore M, Ahmed A, le Noble F. Flt1 acts as a negative regulator of tip cell formation and branching morphogenesis in the zebrafish embryo. *Development.* 2011; 138:2111–2120. [PubMed: 21521739]
52. Myers C, Charboneau A, Cheung I, Hanks D, Boudreau N. Sustained expression of homeobox d10 inhibits angiogenesis. *Am J Pathol.* 2002; 161:2099–2109. [PubMed: 12466126]
53. Searle J, Mockel M, Gwosc S, Datwyler SA, Qadri F, Albert GI, Holert F, Isbruch A, Klug L, Muller DN, Dechend R, Muller R, Vollert JO, Slagman A, Mueller C, Herse F. Heparin strongly induces soluble Fms-like tyrosine kinase 1 release in vivo and in vitro—brief report. *Arterioscler Thromb Vasc Biol.* 2011; 31:2972–2974. [PubMed: 21979436]
54. Drewlo S, Levytska K, Sobel M, Baczyk D, Lye SJ, Kingdom JC. Heparin promotes soluble vegf receptor expression in human placental villi to impair endothelial vegf signaling. *J Thromb Haemost.* 2011; 9:2486–2497. [PubMed: 21981655]
55. Zeng H, Dvorak HF, Mukhopadhyay D. Vascular permeability factor (VpF)/vascular endothelial growth factor (VEGF) receptor-1 down-modulates VpF/VEGF receptor-2-mediated endothelial cell proliferation, but not migration, through phosphatidylinositol 3-kinase-dependent pathways. *J Biol Chem.* 2001; 276:26969–26979. [PubMed: 11350975]
56. Jongen-Lavrencic M, Sun SM, Dijkstra MK, Valk PJ, Lowenberg B. MicroRNA expression profiling in relation to the genetic heterogeneity of acute myeloid leukemia. *Blood.* 2008; 111:5078–5085. [PubMed: 18337557]
57. Maynard SE, Min JY, Merchan J, Lim KH, Li J, Mondal S, Libermann TA, Morgan JP, Sellke FW, Stillman IE, Epstein FH, Sukhatme VP, Karumanchi SA. Excess placental soluble Fms-like tyrosine kinase 1 (sFlt1) may contribute to endothelial dysfunction, hypertension, and proteinuria in preeclampsia. *J Clin Invest.* 2003; 111:649–658. [PubMed: 12618519]
58. Hiratsuka S, Nakamura K, Iwai S, Murakami M, Itoh T, Kijima H, Shipley JM, Senior RM, Shibuya M. MMP9 induction by vascular endothelial growth factor receptor-1 is involved in lung-specific metastasis. *Cancer Cell.* 2002; 2:289–300. [PubMed: 12398893]

Novelty and Significance

What Is Known?

- The formation of new blood vessels is essential for proper embryonic development and progression of diseases, including cancer, and retinopathy.
- Angiogenesis relies on a tightly orchestrated network of attractants and repellants controlling the angiogenic potential of endothelial cells, including VEGFs and their corresponding receptors.
- Post-transcriptional fine-tuning by microRNAs can modulate cellular behavior by titrating doses of proteins generated from mRNAs.

What New Information Does This Article Contribute?

- Reduction of miR-10 results in severely impaired angiogenic behavior of endothelial cells in vivo in zebrafish and in human endothelial cells in vitro.
- miR-10 directly binds to and regulates the expression of the VEGF sequestering VEGF receptor 1 (FLT-1) and its soluble splice variant sFLT-1.
- A reduction of miR-10 results in an increase in FLT-1 protein, which in turn antagonizes pro-angiogenic signaling mediated by VEGF receptor 2 (KDR). Thus, miR-10 promotes VEGF-dependent signaling by negatively titrating FLT1.

In the present study we demonstrate how anti-angiogenic FLT1 and pro-angiogenic KDR signaling is regulated in a miRNA-mediated manner and thereby modulate the behavior of endothelial cells during angiogenesis. We show that knockdown of miR-10 in vivo in zebrafish causes severe defects during embryonic angiogenesis with stalled intersegmental vessel growth. Additionally, we demonstrate that reduction of miR-10 function significantly impairs the angiogenic behavior of human endothelial cells. We provide evidence that miR-10 directly regulates the level of the VEGF sequestering receptor FLT-1 and its soluble splice variant sFLT-1, thereby promoting pro-angiogenic signaling mediated by KDR. Our findings have potential impact diseases involving increased or decreased angiogenesis and implicate miR-10 as a novel target for the selective modulation of angiogenesis.

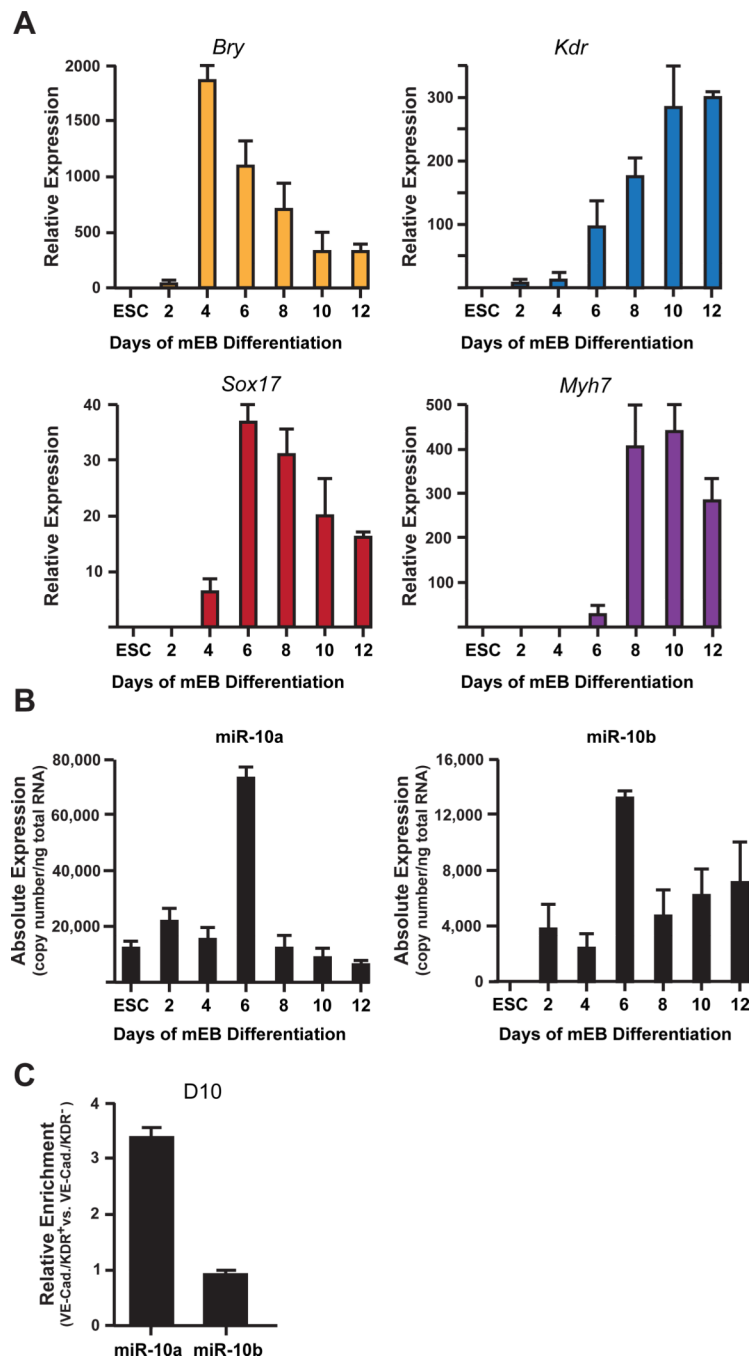


Figure 1. miR-10 is expressed in endothelial cells
qRT-PCR studies of **A**, Marker gene expression during mESC differentiation into EBs; **B**, Absolute expression levels of miR-10a and miR-10b in differentiating EBs; **C**, Relative levels of miR-10a and miR-10b in VE-cadherin⁺/KDR⁺ vs. VE-cadherin⁻/KDR⁻ cells in day 10 EBs. Values are displayed as means \pm SD, * p <0.05; n =4.

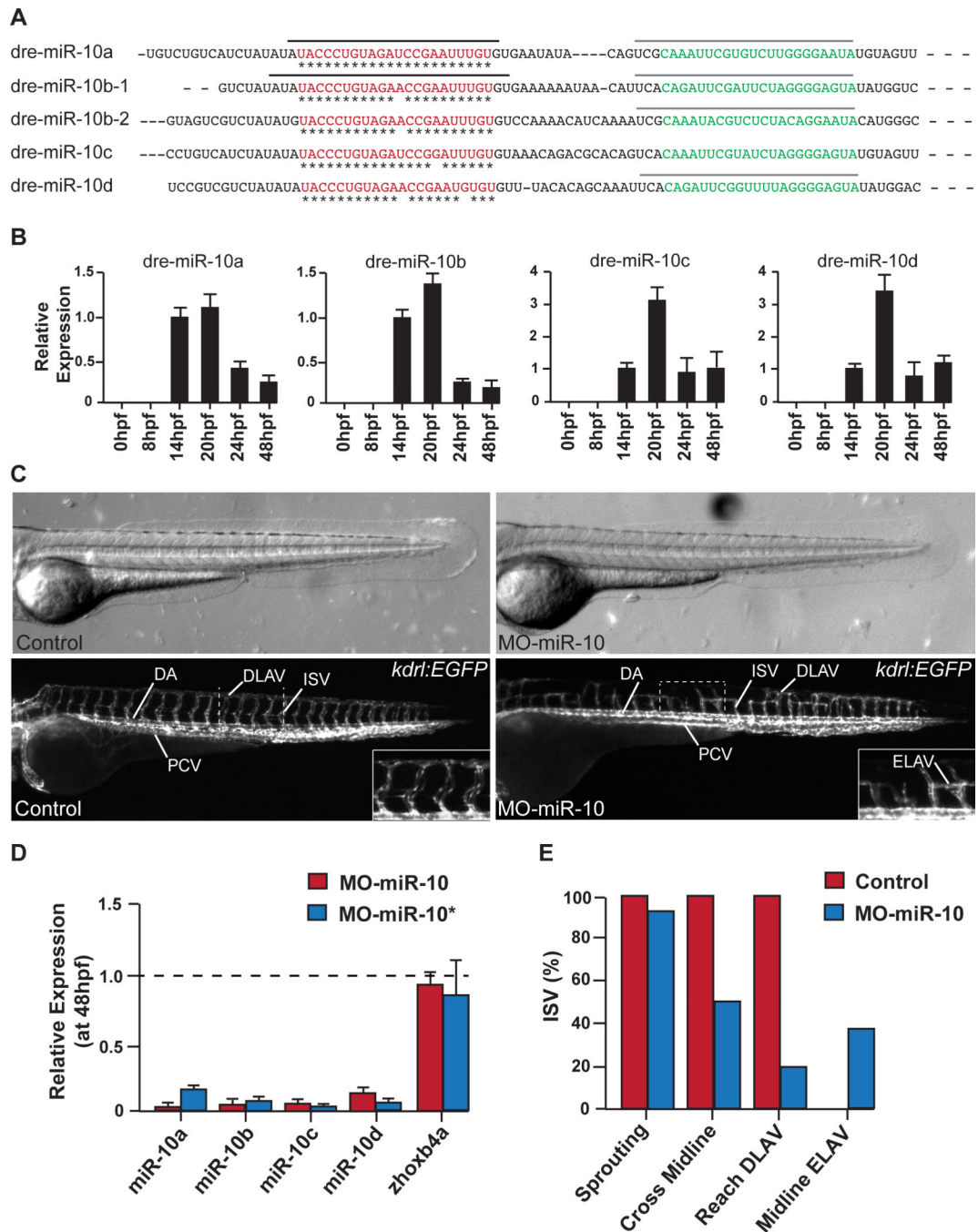


Figure 2. Knockdown of miR-10 leads to defects in vascular development in zebrafish

A, Schematic representation of morpholino (MO) location (black bars for MO-miR-10, grey bars for MO-miR-10*) within the precursor used to target miR-10 processing into mature miR-10 (red letters) and mature miR-10* (grey letters) in zebrafish. **B**, Expression of the different miR-10 isoforms during zebrafish development assayed by qRT-PCR. **C**, Lateral brightfield (top) and fluorescent (bottom) images of *Tg(kdr:EGFP)^{s843}* control-injected and MO-miR-10-injected embryos at 72 hpf. Brightfield images (top) revealed no overall morphological changes upon miR-10 knockdown. Fluorescent images (bottom) showed severe angiogenesis defects. DA, dorsal aorta; DLAV, dorsal longitudinal anastomotic

vessel; ELAV, ectopic longitudinal anastomotic vessel; ISV, intersegmental vessel; PCV, posterior cardinal vein. **D**, Relative expression of genes assessed by qRT-PCR in MO-miR-10 or MO-miR-10* injected embryos at 48 hpf compared to age-matched control-injected embryos. **E**, Quantification of individual ISV phenotypes (n=200, 25 embryos) based on initiation of vessel sprouting from the dorsal aorta (sprouting), vessel crossing the ventral-dorsal midline (cross midline), formation of DLAV (reach DLAV) and formation of premature ELAV in the ventral-dorsal midline (midline ELAV).

\$watermark-text

\$watermark-text

\$watermark-text

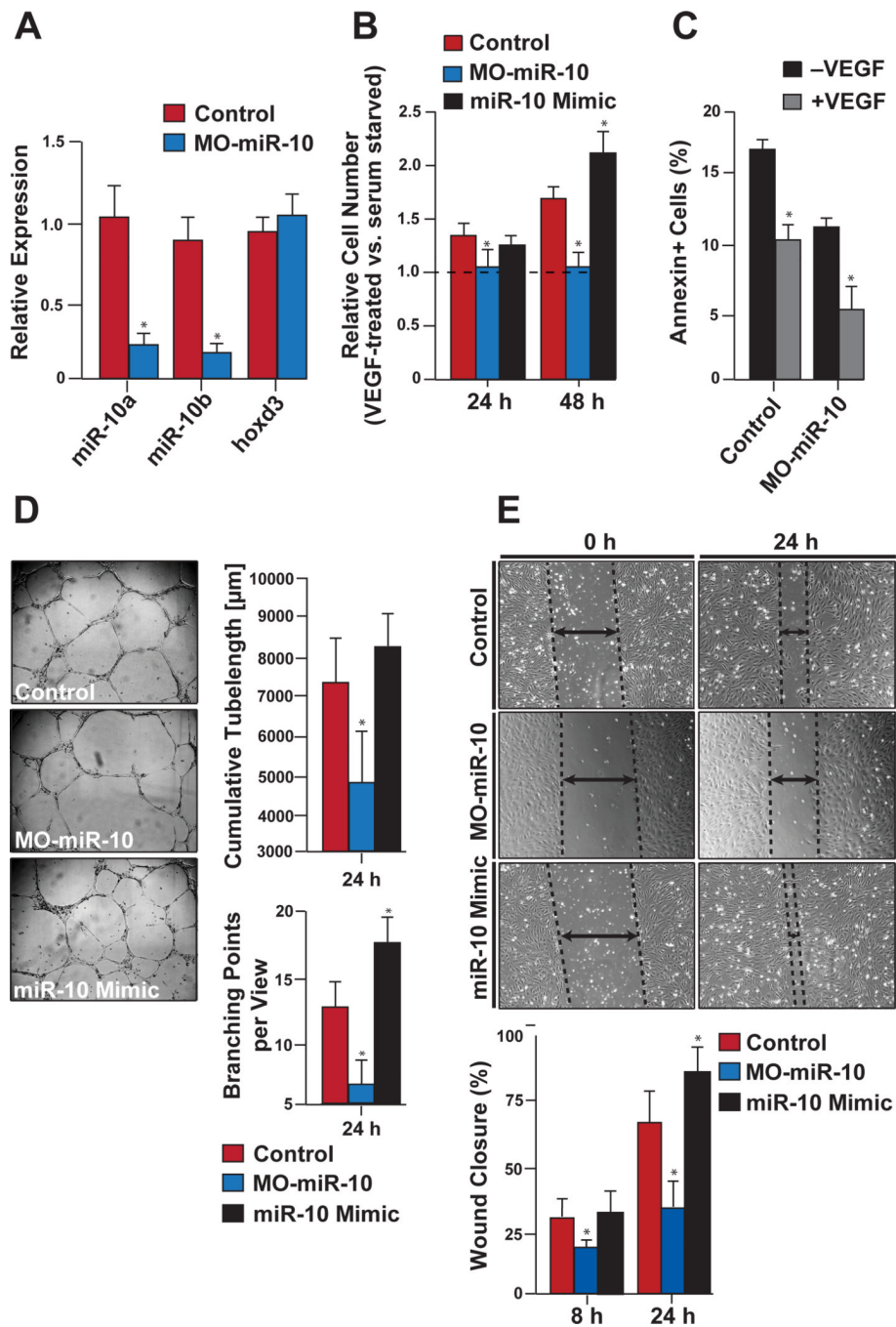


Figure 3. miR-10 affects human endothelial cell behavior in vitro

A, Relative levels of miR-10a, miR-10b and hoxd3 by qPCR 48h after electroporation of MO-miR-10 compared to control-transfected HUVECs. **B**, Changes in cell number in response to VEGF (10ng/ml) assayed in control, MO-miR-10, or miR-10-mimic-transfected HUVECs (* $p < 0.05$ compared to controls). **C**, Annexin V staining of control- or MO-miR-10-transfected HUVECs. **D**, Analysis and images taken following capillary tube formation assay of HUVECs (20x magnification) (* $p < 0.05$ compared to controls, $n = 3$). **E**, Endothelial cell migration of control-, MO-miR-10-, or miR-10-mimic-transfected HUVECs in response to VEGF (10 ng/ml) determined using a scratch assay. Dashed lines indicate

width of gap. Representative images at time of generating scratch (0 h) and 24 h after are shown. Percent wound closure at 8 and 24 h after scratch is shown. Values in graphs are shown as means \pm SD. * $p < 0.05$, $n = 5$.

\$watermark-text

\$watermark-text

\$watermark-text

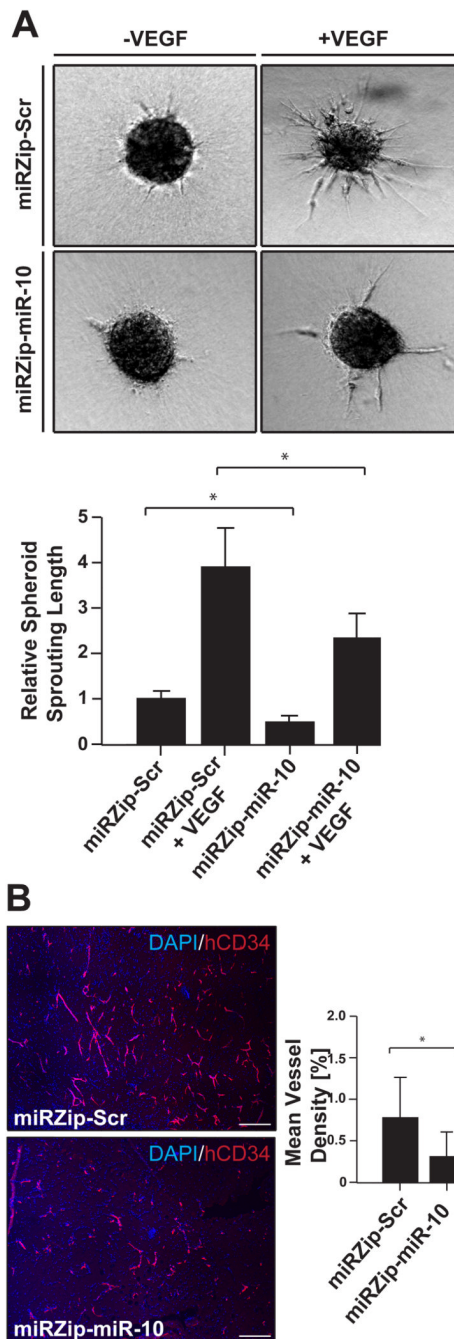


Figure 4. Reduced miR-10 function interferes with angiogenesis

A, Representative pictures of HUVECs infected with a scrambled control lentivirus (miRZip-Scr) and a lentiviral construct designed to specifically block miR-10 for 24 h, followed by a spheroid assay. Quantification of relative cumulative sprout length is displayed (n=5). **B**, Vessel-network formation of miRZip-Scr- or miRZip-miR-10-transduced HUVECs in a Matrigel xenografting assay. Sections (0.5µm) were stained for human CD34 (red) and co-stained with DAPI (blue) and whole matrigel plugs were analyzed for mean vessel density (p<0.05; n=30 from 5 independent mouse experiments).

Representative pictures from regions of high vessel density selected from whole matrigel plugs are shown. Scale bar: 200 μ m.

\$watermark-text

\$watermark-text

\$watermark-text

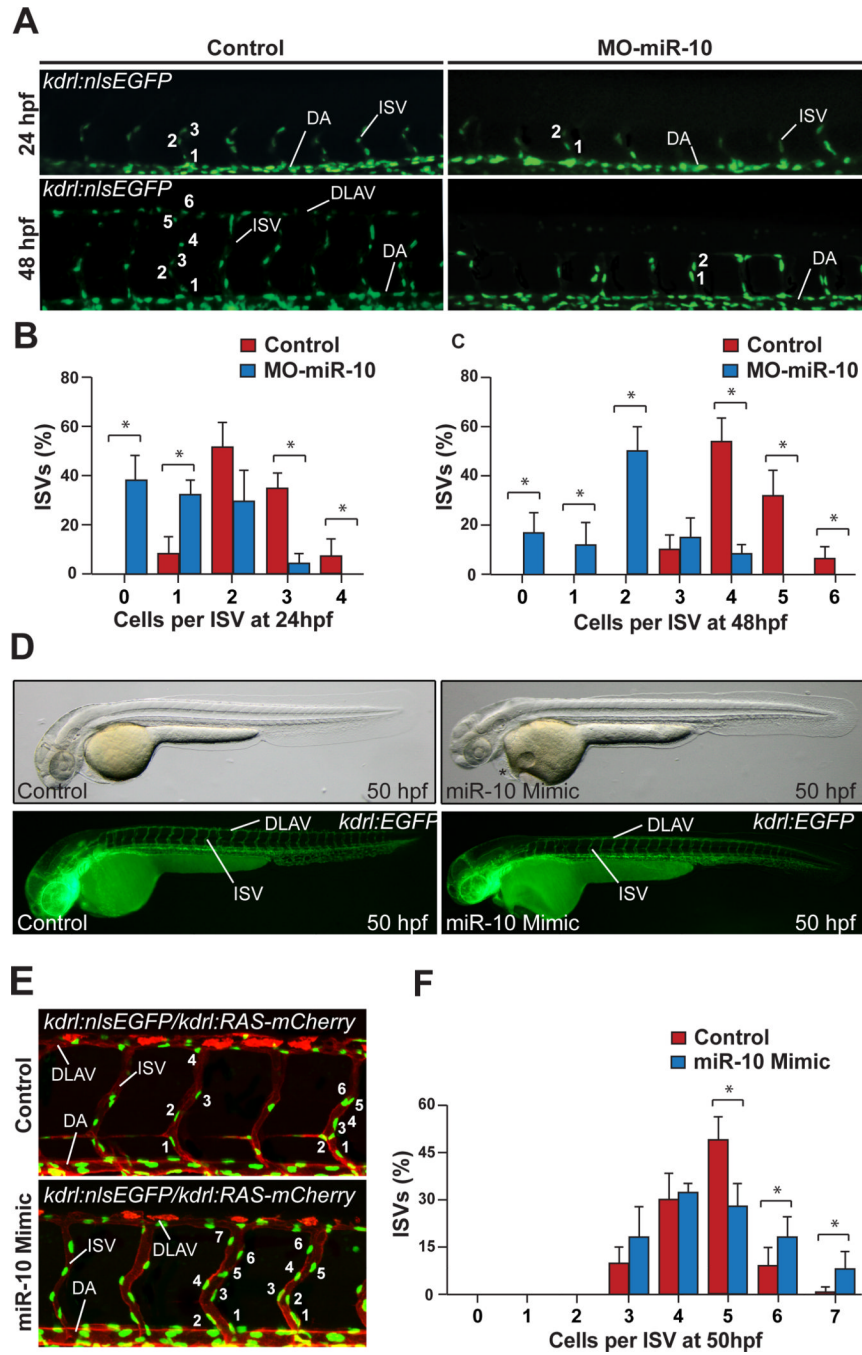


Figure 5. miR-10 regulates endothelial cell division and migration in vivo

A, Proper addition of endothelial cells and migrational behavior of individual cells during dorsal migration of ISVs in control and MO-miR-10-injected embryos was assayed in *Tg(kdr1:nlsEGFP^{zfl109}; kdr1:HsHRAS-mCherry^{s896})* transgenic zebrafish. Images are representative lateral views of 24 hpf or 48 hpf control- or MO-miR-10-injected embryos; numbers indicate endothelial cells in ISVs. DA, dorsal aorta; DLAV, dorsal longitudinal anastomotic vessel; ISV, intersegmental vessels. **B**, Percent of ISVs with indicated cells/ISV in control- or MO-miR-10-injected embryos at 24 hpf. **C**, Percent of cells/ISV in control- or MO-miR-10 injected embryos at 48 hpf. (n= 200 individual ISVs from 25 randomly

selected larvae per condition). **D**, Lateral views of *Tg(kdr1:EGFP)^{s843}* control- or miR-10-mimic-injected embryos at 50 hpf. Besides pericardial edema (asterix), brightfield images (top) revealed no overall morphological changes upon miR-10 knockdown. Fluorescent images (bottom) show normal overall angiogenesis upon miR-10 overexpression compared to control larvae. **E**, Representative confocal images of *Tg(kdr1:nlsEGFP^{zf109}; kdr1:HsHRAS-mCherry^{s896})* transgenic control- and miR-10-mimic-injected zebrafish larvae at 50 hpf. **F**, Percent of cells/ISV in control- or miR-10-mimic-injected embryos at 50 hpf. DA, dorsal aorta; DLAV, dorsal longitudinal anastomotic vessel; ISV, intersegmental vessel.

\$watermark-text

\$watermark-text

\$watermark-text

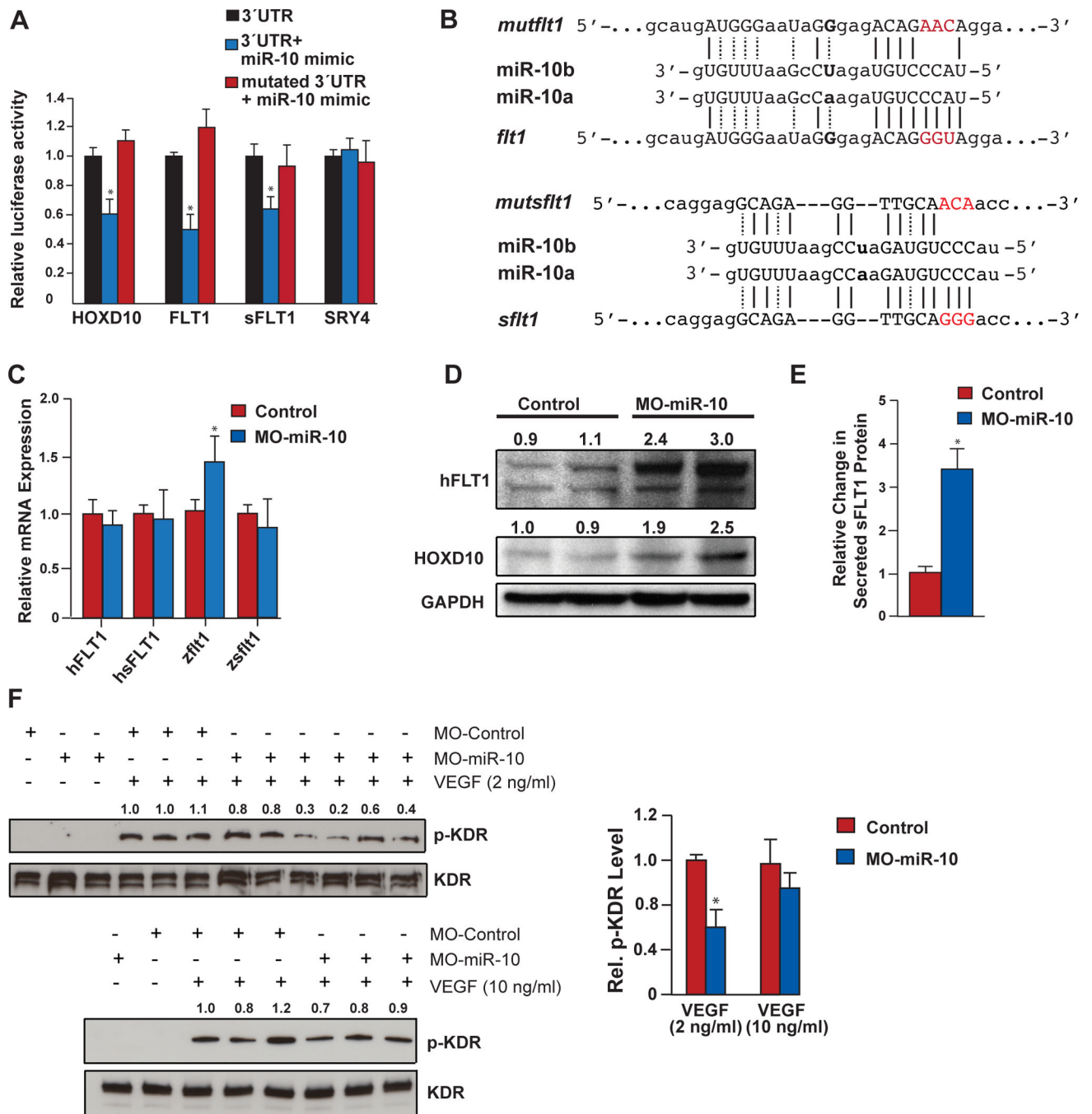


Figure 6. miR-10 directly targets FLT1 and sFLT1 to regulate KDR activity

A, Relative luciferase activity of constructs containing 3'UTRs of indicated genes, with or without mutation of putative miR-10 binding site, and with or without miR-10 mimic in COS-7 cells. HOXD10 was used as a positive control. Values displayed as mean \pm SD, n=3. *p<0.05 compared to 3'UTR alone. **B**, Target-site complementarity between miR-10 and human FLT1 or sFLT1 3'UTR, and sequence of mutation in putative miR-10 binding site in FLT1 3'UTR. **C**, Relative mRNA levels of human (h) and zebrafish (z) flt1/sflt1 in control or miR-10-deficient HUVECs or zebrafish, respectively. *p<0.05 compared to control. **D**, Western blot and densitometric analysis of human FLT1 protein from control or MO-

miR-10-transfected endothelial cells 72 h after transfection. GAPDH was used as a loading control. **E**, Relative change in secreted sFLT1 protein in the supernatant of control or MO-miR-10-transfected HUVECs assessed by ELISA (* $p < 0.05$; $n = 3$). **F**, Immunoblot and analysis of KDR phosphorylation (p-KDR) in HUVECs subjected to low (2 ng/ml) or high (10 ng/ml) concentrations of VEGF (* $p < 0.05$; $n = 6$).

\$watermark-text

\$watermark-text

\$watermark-text

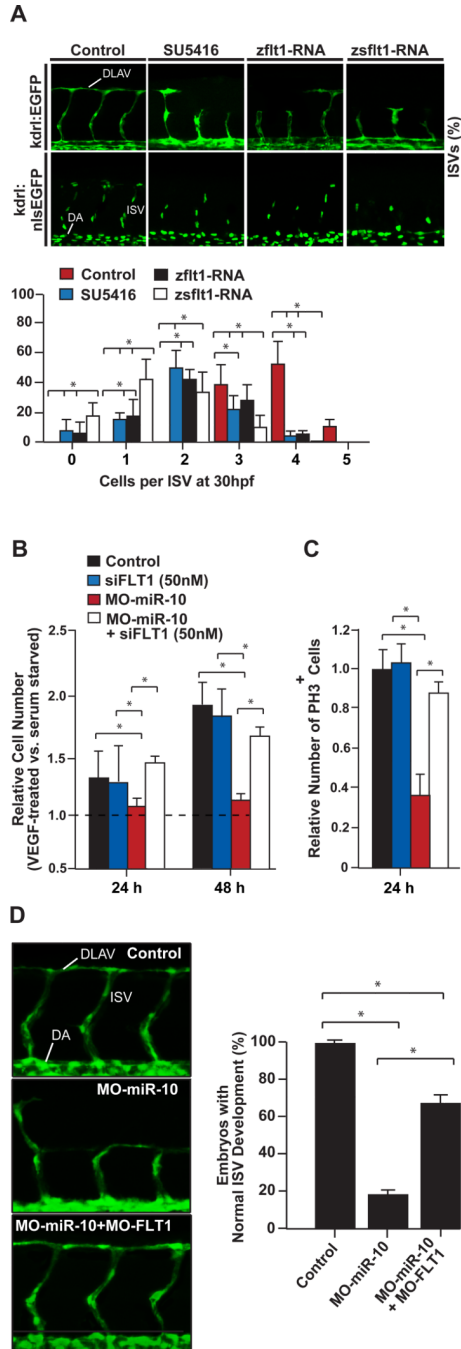


Figure 7. Decreased KDR signaling phenocopies miR-10 deficiency

A, Partial inhibition of KDR signaling in zebrafish (30hpf) by 0.25 μ M SU5416 results in ISV defects similar to miR-10 deficiency. Images are representative high-magnification views. Percent of ISVs with indicated cells/ISV is shown below. Injection of zebrafish *flt1* or *sflt1* mRNA also resulted in angiogenic defects similar to miR-10-deficiency. 200 ISVs from 25 randomly picked larvae per condition were analyzed. DA, dorsal aorta; DLAV, dorsal longitudinal anastomotic vessel. **B**, Relative number of HUVECs in VEGF-treated vs. serum-starvation conditions. Control siRNA effects are shown. * $p < 0.05$, $n = 3$. **C**, Relative number of phosphohistone H3 (PH3)-positive cells following VEGF treatment. * $p < 0.05$,

n=3. **D**, High-magnification view of representative ISVs in 30 hpf *Tg(kdr:EGFP)^{s843}* zebrafish showing partial rescue of MO-miR-10-induced defects in angiogenesis upon injection with a morpholino targeting zebrafish *flt1* (MO-FLT1). Quantification of ISV defect is shown. * $p < 0.05$, n=150 (Control), 185 (MO-miR-10) and 196 (MO-miR-10+MO-FLT1).

\$watermark-text

\$watermark-text

\$watermark-text